Investigation on the Correlation of Stability, Reactivity, and Structural Properties of C/C_2-doped Neutral and Charged Al_n (n=2-7) Clusters

Ramesh Jarupula[a] Surajit Maity[a]*

[a]Department of Chemistry, Indian Institute of Technology Hyderabad, Kandi, Sangareddy, India, PIN-502284
* surajitmaity@chy.iith.ac.in

ABSTRACT: The computational investigation on the equilibrium geometries, electronic structures, reactivity, and stability of C/C_2-doped $Al_n^{0,\pm}$ (n=2-7) clusters at B3LYP-D4/def2-TZVPP level of theory. The lowest energy structures of $Al_nC_{1,2}^{0,\pm}$ clusters are more stable when the carbon atoms are inserted in the aluminium cluster. The stability of the clusters was determined by various parameters such as binding energies, dissociation reaction energies, a second-order difference of energy, chemical hardness, ionization energy, and electron affinity. The results show the singlet cluster ($Al_{2,4,6}C_{1,2}$ and $Al_{3,5,7}C_{0-2}^{0,\pm}$) shows greater stability than the doublet clusters ($Al_{3,5,7}C_{0-2}$ and $Al_{2,4,6}C_{1,2}^{0,\pm}$) followed by triplet clusters ($Al_{2,4,6}$). The stability of cationic species is less than that of neutral species, but anionic clusters are shown to be more stable than the neutral species. The present study can be significant to know the stability and reactivity of the metal clusters upon carbon doping. Such materials have great importance in combustion, material science, and astrochemical community.

Keywords: Density Functional Theory, Carbon doped aluminium clusters, Structure and stability, Dissociation energy and chemical hardness, Vertical detachment energy and electron affinity, Ionization energy.

1. Introduction

The chemistry of metal clusters is an emerging topic in the fundamental study of molecular and solid-state chemistry that has applications in material science and catalysis.[1][2][3] It is important for the development of novel materials aiming for application in the field of nanocatalysis, metalized fuels, semiconductors, ceramics, etc.[4][5][6] Doping of an atom to pure clusters brings a new dimension to the entire electronic structure and properties of the cluster, opening up new possibilities for the development of innovative materials for technological applications.[7] Aluminium has been applied as a nanoparticle fuel additive to enhance the energy density of the fuel.[8,9] New composite materials of carbon and aluminium have a wide range of applications in the aerospace industry, energetics, and medicine[10]. They are known for their distinguished thermos-luminescence,[11,12] sensing of pollutant gas molecules,[13,14], and semiconducting properties.[15–17] Catalytic activity of C/Al-doped molecules plays a key role in various chemical reactions.[15–17] Al-catalysed water oxidation is one of the widespread chemical reactions.[18–20] The uniqueness of the Al-containing materials lies in the fact that aluminium is a trivalent atom in larger clusters and monovalent in smaller clusters due to the large energy gap between 3s and 3p electronic states.[21] Additionally, Aluminium and carbon-containing smaller molecules have astrochemical significance due to their abundance in the interstellar medium.[22–27]

A systematic comparative investigation of the structure, stability, reactivity, and bonding of charged and neutral clusters of $Al_nC_{1,2}^{0,\pm}$ is limited in the literature. Due to the vast applications of the atom-doped clusters in advanced materials, experimental and theoretical characterization of carbon-doped Al clusters (neutral and anionic) have gained a lot of attention over the last decade. For example, the chemical structure and bonding of various aluminium carbon clusters, such as AlC_2,[28–30] Al_3C,[31] Al_4C^-,[32] Al_5C,[33] Al_2C_2 and $Al_2C_2^-$,[34] $Al_3C_2^-$,[35] and neutral and anionic Al_nC_5 clusters,[36] have been studied by combined photo electronic spectroscopy and theoretical methods. Sugioka et al.[6] and Zhai et al.[37] reported the mass distribution of Al_nC^- clusters carried out by laser ablation experiment aided by the computational investigation. Tsukuda et al. reported the photoelectron spectroscopy of $Al_nC_2^-$ (n = 5−13) as a product of laser-ablated Al_n with various organic molecules.[38] Additionally, theoretical investigations on the structure and bonding of Al_nC clusters suggested the enhanced stability of Al_4C and $Al_{12}C$ clusters compared to their adjacent clusters through DFT calculations.[21] Naumkin et al. reported the electronic structure properties of small aluminium clusters $Al_{2m}C_n$ calculated using the MP2 level of theory.[39] Recently, Loukhovitski et al. reported the physical and thermodynamic properties of Al_nC_m and calculated the reaction energies associated with the Al_n clusters under the combustion condition.[40] Ashman et al. have studied the stability of neutral and anionic Al_nC clusters reacting with O_2.[41] The authors suggest unusually high stability of neutral and anionic Al_7C clusters, which was agreed by an experimental work by Leskiw et al..[42] The Al-C bonding and electronic structure of selective carbon-doped clusters, such as $Al_{4,6}C_{1-4}$, were investigated.[43–46]

In spite of experimental and computational reports, the structures of neutral and charged $C_{1,2}$-doped Al_n species with n>3 remained uncertain to date. In this article, we have discussed the bonding in the structures of the neutral, cationic, and anionic clusters using relevant parameters, such as bond lengths and HOMO-LUMO interactions. The stability of the clusters was discussed using the incremental binding energy and second-order difference of energy, dissociation energies (DE). Note that, under various experimental conditions, such as laser ablation and resistively heated graphite tube, the molecular abundance of a series of clusters, Ge_n, Si_n, B_n, AlB_n, Au_n, Au_nPt_m[47–49], was found to be correlated with the second-order difference of energy (Δ^2E). In the current systems, the (Δ^2E) can be calculated as the reaction energy of $2Al_nC_{1,2} \rightarrow Al_{n+1}C_{1,2} + Al_{m-1}C_{1,2}$, i.e., $\Delta^2E = E(Al_{n+1}C_{1,2}) + E(Al_{n-1}C_{1,2}) - 2E(Al_nC_{1,2})$. The reactivity of the above was discussed using the relevant parameters, such as chemical hardness (η), and HOMO-LUMO bandgap energy (E_{HL}) values, ionization energy parameters. Among the charged species, the anionic clusters, $Al_nC_{1,2}^-$, has been the main interest of the spectroscopy community. Under similar experimental conditions, the formation of the respective cationic species is equally feasible. Therefore, the stability and bonding in the cationic species $Al_nC_{1,2}^+$ are discussed in detail. The current study will facilitate the fundamental bonding interaction between Al-C, which also help in understanding the growth mechanism of similar nanoparticles. The current study will be beneficial to understand the factors affecting the bonding and stability of the key intermediates in C-H activation and metal insertion reactions in organometallic chemistry.

2. Methods

The geometry optimization of the neutral and charged Al_nC_m molecular species were performed using the TURBOMOLE program package.[50] The calculations were done using the B3LYP-D4/def2-TZVPP level of theory.[51] The optimization criteria were set with a smaller grid size (m5) and low convergence criteria (10^{-6} Hartree/Bohr). The B3LYP level proved to be an efficient method to study aluminium carbon clusters, as reported earlier.[5,36] The optimized geometries were confirmed with all positive harmonic vibrational frequencies. Single point energies were calculated to determine the vertical ionization energies, vertical electron affinities, and vertical detachment energies of the clusters. The binding energies ΔE were calculated as $\Delta E(Al_nC_m) = E(Al_nC_m) - n*E(Al)-m*E(C)$. Dissociation energies of several low-energy reaction channels, incremental binding energy, and second-order difference of energy values were calculated to study the stability of the molecules. In addition, the vertical and adiabatic ionization energy (VIE and AIE), electron affinity (VEE and AEE), vertical electron detachment energy (VDE), chemical hardness (η) of the molecules, HOMO-LUMO energy gaps were calculated to investigate the reactivity of the clusters. Only the most stable structures are presented in this article. The other isomers of each molecule have also been studied and are given in the supporting information document.

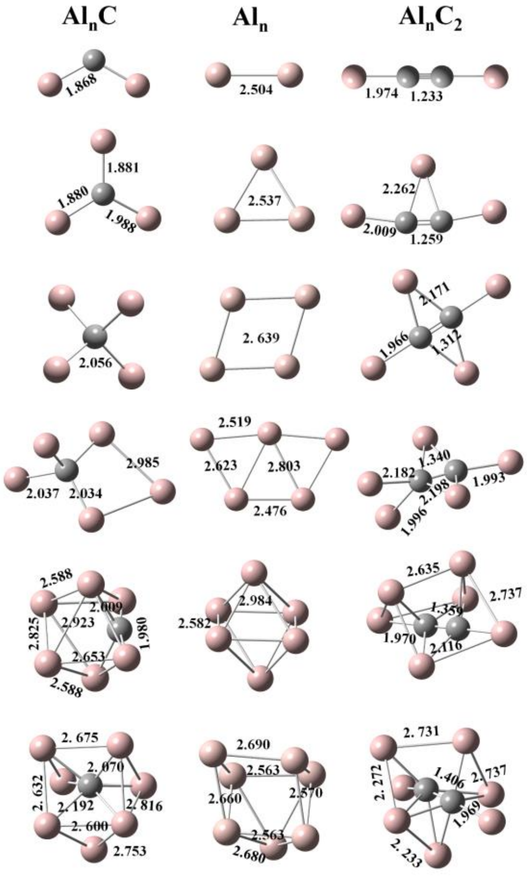

Figure 1: Ground state optimised geometries of C and C_2 doped neutral Al_n (n=2-7) clusters and structural parameters calculated at B3LYP-D4/def2-TZVPP level of theory.

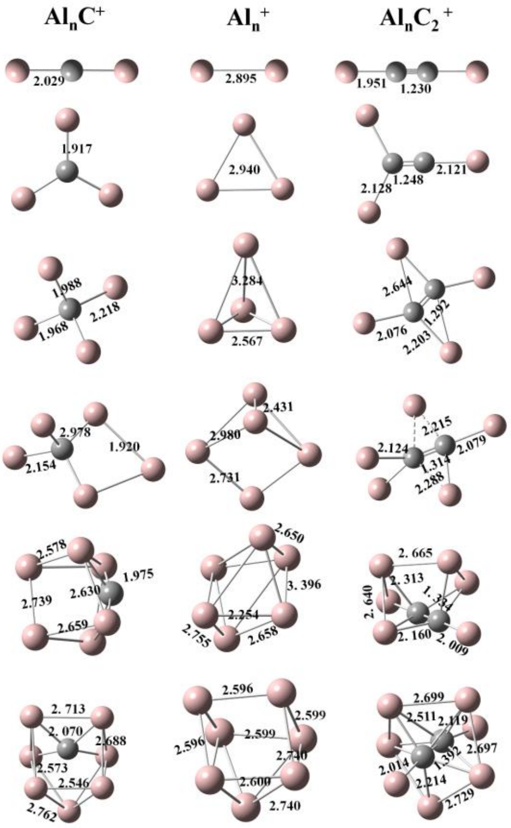

Figure 2: Ground state optimised geometries of C and C_2 doped cationic Al_n (n=2-7) clusters and structural parameters calculated at B3LYP-D4/def2-TZVPP level of theory.

3. Results and Discussion

3.1 Structures and Bonding

Detailed investigations on the geometries of the most stable Al_{2-7} clusters in the neutral, cationic, and anionic forms and the structures are reported in the literature.[52][53] A brief discussion on the clusters was given here to validate the present level of the computational method. The geometry-optimized structures of Al_{2-7} were extensively searched across various spin multiplicities. The lowest energy Al_n structures of the neutral clusters are shown in Figure 1. The average binding energy, symmetry, electronic ground state, and vibrational frequencies of the lowest energy structures are presented in Table 1. The lowest energy structures of the even Al-clusters, i.e., $Al_{2,4,6,}$ have $D_{\infty h}$ (triplet), D_{2h} (triplet), and C_{3v} (singlet) symmetries, respectively. The D_{3d} symmetric Al_6, which was previously reported by Kim et al. and Tan et al.,[52][53] as shown in Figure 1, is found to be marginally less stable (0.032 eV) than a C_{3V} symmetric structure shown in SI Table S1. The former structure is used for further analysis. The lowest energy structures of the $Al_{3,5,7}$ species are found to be D_{3h} (doublet), C_{2v} (doublet), and C_{3v} (doublet) symmetries, respectively, similar to that reported earlier.[52][53] The Al_{4-7} structures possess a nearly planner four-membered ring, and the additional Al-atom(s) in Al_5 and Al_{6-7} structures are positioned on the edge and face of that plane, respectively. The structures of Al_{4-6}^+ are found to be different than that of the neutral species, with C_{3V} for n=4, C_{2V} for n=5, and C_s for n=6 (Figure 2), respectively. In the case of anionic cluster Al_{2-7}^- (Figure 3), the most stable structures are found to have a nearly similar geometry as the neutral counterparts. All the above neutral, cationic, and anionic structures are found to be identical to that reported earlier.[52] The average Al-Al bond length in the cations are longer than the neutral species, suggesting the weakening of Al-Al bonds upon ionization. However, in the anionic species, the smaller Al-Al bond lengths suggest higher stability of the anionic clusters.

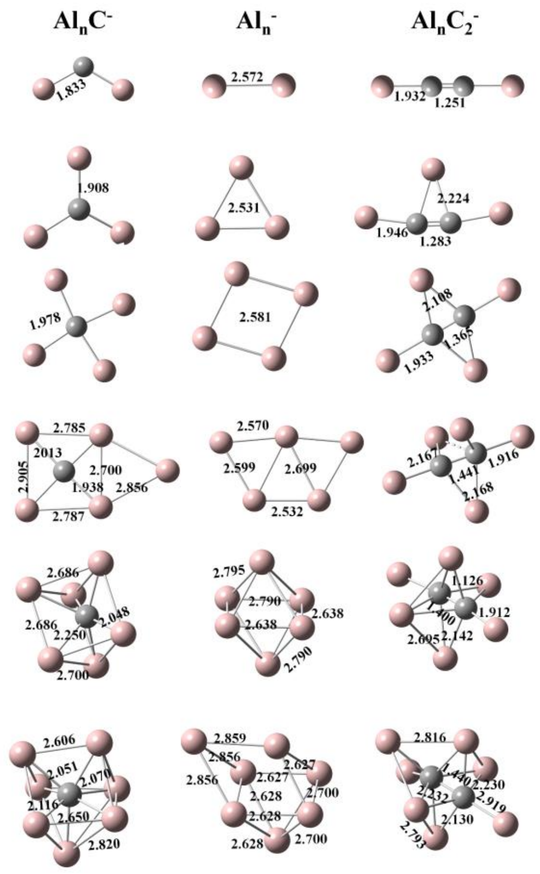

Figure 3: Ground state optimised geometries of C and C_2 doped anionic of Al_n (n=2-7) clusters and structural parameters calculated at B3LYP-D4/def2-TZVPP level of theory.

3.1.1 Structures of $Al_nC_{1,2}^{0,\pm}$ Clusters

The neutral Al_n structures were doped with the $C_{1,2}$ units at the (a) center, (b) faces, and (c) edges, and the geometry optimized most stable $Al_{2\text{-}7}C_{1,2}$ clusters were shown in Figure 1. The structures of other higher energy isomers with relative energies (ΔE_r) ranging within 1.0 eV were given in SI Table S1. The lowest energy structures of the cationic $Al_nC_{1,2}^+$ and anionic $Al_nC_{1,2}^-$ are shown in Figures 2 and 3, respectively. The average binding energy values symmetry and electronic ground state and the vibrational frequencies of the lowest energy structures were presented in Table 1.

Table 1: Structural parameters average binding energy E_b in eV, vibrational frequencies in cm^{-1}, ground electronic states and symmetry of the most stable $Al_n^{0,\pm}$, $Al_nC^{0,\pm}$ and $Al_nC_2^{0,\pm}$ (n=1-7)

E_b (eV)$^\#$	**Structural parameters**	**E_b (eV) $^\#$**	**Structural parameters**	**E_b (eV) $^\#$**	**Structural parameters**
-0.66	**l-Al_2 ($^3\Pi_u$); $D_{\infty h}$**	2.44	**l-Al_2^+($^2\Sigma_g^+$); $D_{\infty h}$**	-1.28	**l-Al_2^- ($^2\Sigma_g^-$); $D_{\infty h}$**
-1.13	**Al_3($^2A_1'$); D_{3h}**	0.93	**Al_3^+($^3A_1'$); D_{3h}**	-1.62	**Al_3^-($^1A_1'$); D_{3h}**
-1.30	**Al_4($^3A_{1g}$); D_{2h}**	0.22	**Al_4^+($^4A_1$); C_{3v}**	-1.80	**Al_4^-($^2A_{1u}$); D_{2h}**
-1.50	**Al_5($^2A_1$); C_{2v}**	-0.29	**Al_5^+($^1A_1$); C_{2v}**	-1.88	**Al_5^-($^1A_1$); C_{2v}**
-1.69(-1.69)	**Al_6($^1A_1$); C_{3v} (D_{3d})**	-0.64	**Al_6^+(^2A); C_s**	-2.02	**Al_6^-($^2A_{1g}$); D_{3d}**
-1.85	**Al_7($^2A_1$); C_{3v}**	-1.05	**Al_7^+($^1A_1$); C_{3v}**	-2.12	**Al_7^-($^1A_1$); C_{3v}**
-1.69	**l-AlC ($^4\Sigma_u^+$); $C_{\infty v}$**	2.62	**l-AlC^+ ($^3\Sigma_g^+$); $C_{\infty v}$**	-2.04	**l-AlC^- ($^3\Pi_g^+$), $C_{\infty v}$**
-2.21	**c-Al_2C ($^3A_1$); C_{2v}**	0.12	**l-Al_2C^+ ($^4\Pi_g^+$); $D_{\infty h}$**	-2.80	**c-Al_2C^- ($^2\Pi_u^-$); C_{2v}**
-2.61	**Al_3C ($^2A_1$); C_{2v}**	-0.94	**Al_3C^+($^3A_1'$); D_{3h}**	-3.16	**Al_3C^- ($^1A_1'$); D_{3h}**
-2.62	**Al_4C ($^1A_1$); T_d**	-1.23	**Al_4C^+($^2A'$); C_s**	-2.94	**Al_4C^- ($^2A_1$); D_{2d}**
-2.43	**Al_5C (^2A); C_1**	-1.47	**Al_5C^+($^1A_1$); C_{2v}**	-2.80	**Al_5C^- ($^1A_1$); C_{2v}**
-2.41	**Al_6C (^1A); C_2**	-1.51	**Al_6C^+(^2A); C_2**	-2.73	**Al_6C^- ($^2A'$); C_s**
-2.44	**Al_7C ($^2A'$); C_s**	-1.64	**Al_7C^+(^1A); C_1**	-2.79	**Al_7C^- ($^1A_1$); C_{3v}**
l-C_2 ($^1\Sigma_g^+$); $D_{\infty h}$		**l-C_2^+($^2\Pi_g$); $D_{\infty h}$**		**l-C_2^- ($^2\Sigma_g^+$); $D_{\infty h}$**	
-3.04	$\upsilon_{C\text{-}C}$: 1876	3.58	$\upsilon_{C\text{-}C}$:1595	-4.61	$\upsilon_{C\text{-}C}$:1854
c-AlC_2 ($^2A_1$); C_{2v}		**c-AlC_2^+($^3A_1$), C_{2V}**		**l-AlC_2^- ($^1\Sigma$), $C_{\infty v}$**	
-3.75	$\upsilon_{C\text{-}C}$: 1802	-0.65	$\upsilon_{C\text{-}C}$: 1814	-4.56	$\upsilon_{C\text{-}C}$: 1856
l-Al_2C_2 ($^1\Sigma_g^+$); $D_{\infty h}$		**l-$Al_2C_2^+$ ($^2\Pi$); $D_{\infty h}$**		**l-$Al_2C_2^-$ ($^2\Pi_g$); $D_{\infty h}$**	
-3.87	$\upsilon_{C\text{-}C}$:2090	-1.94	$\upsilon_{C\text{-}C}$:2095	-4.06	$\upsilon_{C\text{-}C}$:1930
Al_3C_2($^2A'$); C_s		**$Al_3C_2^+$($^1A_1$); C_{2v}**		**$Al_3C_2^-$($^1A_1$); C_{2v}**	
-3.43	$\upsilon_{C\text{-}C}$:1875	-2.26	$\upsilon_{C\text{-}C}$:1936	-3.79	$\upsilon_{C\text{-}C}$: 1735
Al_4C_2 ($^1A_{1g}$); D_{2h}		**$Al_4C_2^+$(^2A_u); C_{2h}**		**$Al_4C_2^-$($^2A_{1u}$); D_{2h}**	
-3.31	$\upsilon_{C\text{-}C}$:1609	-2.21	$\upsilon_{C\text{-}C}$: 1630	-3.57	$\upsilon_{C\text{-}C}$: 1371
Al_5C_2 (^2A); C_1		**$Al_5C_2^+$(^1A); C_2**		**$Al_5C_2^-$($^1A_1'$); D_{3h}**	

-3.05	υ_{C-C}: 1404	-2.21	υ_{C-C}:1534	-3.42	υ_{C-C}: 1180
Al_6C_2 (^1A); C_2		**$Al_6C_2^+$(^2A); C_2**		**$Al_6C_2^-$(^2A); C_1**	
-3.01	υ_{C-C}:1353	-2.19	υ_{C-C}: 1471	-3.25	υ_{C-C}:1294
Al_7C_2 (^2A); C_1		**$Al_7C_2^+$(^1A); C_1**		**$Al_7C_2^-$($^1A'$); C_s**	
-2.90	υ_{C-C}:1221	-2.27	υ_{C-C}: 1254	-3.16	υ_{C-C}: 1163

E_b ($Al_nC_m^{0,\pm}$) = E ($Al_nC_m^{0,\pm}$) - n*E(Al)-m*E(C) /(n+m)

The lowest energy structures of $Al_{3-7}C$ clusters possess singlet and doublet ground states for the even and odd n-values, respectively. The C-atom is positioned at the center of the Al_n species (except for Al_6C with the edge-bound carbon atom) in the above structures. The structures obtained by positioning the carbon atom at the edge of the Al_n species mostly resulted in the lower energy isomers with relative energies of 1.85, 0.42, 0.13, and 0.97 eV for n=3, 4, 5, and 7, respectively. As shown in Figure 1, the doping of a carbon atom in Al_2, and Al_3 resulted in a significant increase in Al-Al distance. In the structures, the formation of relatively stronger Al-C bonds (E_b of Al-Al and Al-C are -0.66 and -1.69 eV, respectively) stabilizes the structures. The $Al_{4,5}C$ structure has a tetrahedral C-atom at the center, similar to that reported earlier.[21,41,54] Different structures of $Al_{4,5}C$ (shown in SI Table 1) were reported by Gui-Fa et al.[55], which were found to be 0.42 and 0.18 eV less stable at the current level of theory, respectively. In the case of Al_6C, the lowest energy structure (C_2-symmetric) is found to have the carbon atom inserted in the Al-Al bond at the edge, similar to that reported by Ashman et al..[28] The isomer with C-atom at the center of the Al_6-unit, forming a D_{3h} symmetric structure (similar to that reported in ref. [54]; SI Table S1), is found to be less stable by 0.07 eV. The most stable C_s-symmetric Al_7C structure is found to be similar to that reported earlier.[54]

The C_2-doped Al_n clusters are found to have an insertion of the C_2 unit in the Al_n molecule (Figure 1). As shown in the $Al_{2,3}C_2$ structures, the C_2 unit is inserted within the Al-Al bond. In the case of $Al_{4-7}C_2$, the C_2 is inserted along the long diagonal of the rhombus-shaped Al_4-unit in the Al_n molecules. The structures of $Al_{2-6}C_2$ are similar to the reported lowest energy structures.[5,56,57] The C-C bonds in $Al_{4-7}C_2$ have shown a significant increase in bond length with the increasing size of the clusters, suggesting the lowering of CC bond orders. The CC stretching frequencies in the above molecules (Table 1) have shown 200-600 cm^{-1} redshift compared to the acetylenic structures found in the Al_2C_2.

The structures of the corresponding cationic species $Al_nC_{1,2}^+$ are shown in Figure 2. Except for Al_5C^+, other cationic structures are not yet reported. The most stable structures of Al_5C^+ were reported as D_{5h} symmetric by Pei et al.[45]. However, at the current level of theory, the lowest energy structure of Al_5C^+ is found to be C_{2v} symmetric, similar to the neutral molecule. The D_{5h} symmetric cluster (SI Table 1) is less stable by 0.240 eV than the C_{2v} structure. The C_{2v} symmetric Al_5C^+ was also reported earlier to be the most stable structure at MP4(SDQ)/aug-cc-pVTZ//MP2/aug-cc-pVTZ and CCSD/aug-cc-pVTZ//MP2/aug-cc-pVTZ levels of theory.[45] The Al_2C^+ structure is found to be linear ($D_{\infty h}$) with a $^4\Pi_g^+$ ground electronic state, which is different from the neutral and anionic structures. The most stable structure of $Al_{3-7}C^+$ having D_{3h}, C_s, C_{2v}, C_2, and C_1 symmetries, respectively, for n=3-7, are found to be marginally different compared to their neutral counterparts. The C_2-doped cationic $Al_nC_2^+$ clusters (Figure 2) with odd and even numbers of Al-atoms show singlet and doublet ground states, respectively. The most stable structures of $Al_{3,4,5}C_2^+$ with C_{2v}, C_{2h}, and C_2 symmetries, respectively, are found to be different compared to their neutral counterparts with C_s, D_{2h}, and C_1 symmetries. However, the most stable structures of $Al_{6,7}C_2^+$ are found to be similar to the respective neutral species.

Figures 3 depict the structures of the anionic species, $Al_nC_{1,2}^-$. The most stable Al_2C^- structure was found to be similar to the neutral structure with C_{2v} symmetry. The most stable structures of $Al_{3-7}C^-$ are different from their neutral counterparts with D_{3h}, D_{2d}, C_{2v}, C_s, and C_{3v} symmetries, respectively. The even and odd number of aluminum-containing clusters possess doublet and singlet states. The Al_3C^- and Al_5C^- structures are similar to the cationic species. All the structures except $Al_{4,5}C^-$ are found to be similar to structures reported by Ashman et al..[28] The reported Al_4C^- with D_{4h} is found to be 0.32 eV less stable than the D_{2d} structure shown in Figure 3. The C_{2V} symmetric AlC_5^- is found to be similar to that reported by Boldyrev et al.[44]

The most stable structures of $Al_nC_2^-$ clusters also possess the singlet and doublet states for odd and even numbers of Al-atoms in the clusters. The $Al_{2,4}C_2^-$ are similar to their neutral geometries having $D_{\infty h}$ and D_{2h} symmetries, whereas the $Al_{3,5-7}C_2^-$ structures with C_{2v}, D_{3h}, C_1, and C_s symmetries, respectively, are different compared to the respective neutral clusters. Cannon et al. reported $Al_2C_2^-$ structure with C_{2h} symmetry is different compared to the $D_{\infty h}$ structure in Figure 3.[34]. The structure of $Al_3C_2^-$ with C_{2v} symmetry is similar to the reported structures.[32,35]

3.2 Stability of the $Al_nC_m^{0,\pm}$ (n=1-7; m=0-2)

The stabilities of the structures were verified based on the following energy parameters: (a) average binding energy, (b) dissociation energy, and (c) chemical hardness.

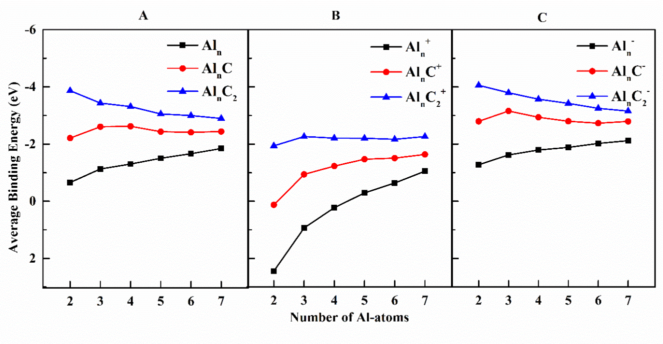

Figure 4: The average binding energies ΔE_b (eV) of the (A) neutral (B) cationic and (C) anionic $Al_nC_{1,2}^{0,\pm}$ clusters

3.2.1 Binding energy

The binding energies ΔE for both neutral and charged Al_nC_m clusters were calculated using the following method: $\Delta E = E(Al_nC_m^{0,\pm}) - n\times E(Al) - m\times E(C)$. The average binding energy E_b is calculated as $\Delta E/n+m$. The lower the value of the average binding energies (E_b), the higher the stability of the structures. The calculated E_b values of the most stable $Al_nC_{0-2}^{0,\pm}$ (n=1-7) clusters are given in Table 1. The variation in the E_b as a function of a number of Al-atoms of the neutral, cationic, and anionic species are shown in Figures 4A, 4B, and 4C, respectively. The more negative E_b values of $Al_nC_{1,2}$ indicate that the doping of carbon increases the stability of the Al_n clusters. It is evident from the structures that some of the Al-Al bonds are replaced by Al-C bonds in Al_nC and Al_nC_2. Therefore, the highly negative E_b values of $Al_nC_{1,2}$ are justified. The additional CC bonds in Al_nC_2 increase

Table 2: Ionization energy (vertical and adiabatic) and electron affinity (vertical and adiabatic), vertical electron detachment energy, HOMO-LIMO energy gaps and chemical hardness (η) of Al_n, Al_nC and Al_nC_2 species in eV. The energies calculated at CCSD(T) method are given in paranthesis.

Name	**VIE (eV)**		**AIE (eV)**		**VEA (eV)**		**AEA (eV)**		**VDE (eV)**		E_{HL}	η
	Calc	**(Expt)**[1]	**Calc**	**(Expt)**[2]	**Calc**	**(Expt)**[3]	**Calc**	**AEA (Expt)**[4]	**Calc**	**VDE (Expt)**[5]		
***l*-Al_2**	6.37	6.0-6.42	6.19	6.20	1.25		1.24	1.46 ± 0.06	1.23	1.60	1.30	3.81
Al_3	6.31	6.42-6.5	6.19	6.45	1.52	1.53	1.47	1.89 ± 0.04	2.19	1.90	1.49	3.91
Al_4	6.47	≥6.5	6.11	6.55	1.97	1.74	1.97	2.20 ± 0.05	2.14	2.20	1.09	4.22
Al_5	6.18	6.42-6.5	6.04	6.45	1.87	1.82	1.90	2.25 ± 0.05	1.87	2.30	1.67	4.02
Al_6	6.53	6.0-6.42	6.17	6.45	1.89	2.09	2.15	2.63 ± 0.06	2.29	2.65	1.77	4.21
Al_7	5.75	6.0-6.42	5.55	6.20	1.68	1.96	1.92	2.43 ± 0.06	2.06	2.50	1.68	3.72
Al_2C	7.24		7.00 (7.68)		1.61		1.76 (2.03)		1.71		1.93	4.43
Al_3C	6.55		6.65 (6.85)		2.30		2.20 (2.51)		2.12	2.56 ± 0.06[6]	1.16	4.42
Al_4C	7.49		6.96 (7.56)		1.08		1.57 (1.42)		1.63	2.65 ± 0.06[7]	2.91	4.29
Al_5C	5.70		5.77 (5.93)		1.64		2.19 (2.76)		2.15	2.67 ± 0.03[8]	1.59	3.67
Al_6C	6.29		6.30 (6.61)		1.85		2.26 (2.24)		2.37		1.89	4.07
Al_7C	6.42		6.42 (6.54)		2.86		2.82 (3.19)		2.80		1.33	4.64
***l*-Al_2C_2**	7.52		7.71 (8.19)		0.93		0.76 (0.54)	0.64[9]	0.59	0.71[9]	3.56	4.22
Al_3C_2	6.55		5.84 (6.00)		1.97		1.81 (2.00)	2.19± 0.03[10]	1.68		1.70	4.26
Al_4C_2	7.40		6.61 (7.14)		1.71		1.55 (1.69)		1.44		2.80	4.55
Al_5C_2	6.02		5.93 (6.08)		2.23		2.60 (3.02)		3.13		1.51	4.13
Al_6C_2	6.57		6.56 (7.01)		1.8o		1.94 (2.33)		2.18		2.63	4.23
Al_7C_2	5.67		5.69 (5.84)		2.28		2.33 (2.71)		2.18		1.41	3.97

Vertical electron detachment energies (VDEs) as determined from the photoelectron spectra. The absolute error of the energies is ±0.1 e

IE and EA calculated at CCSD(T) method.

the stability of the C_2-doped clusters. Similar trends were observed for the cationic $Al_nC_{1,2}^+$ and anionic $Al_nC_{1,2}^-$ clusters, as shown in Figures 4B and 4C, respectively. In the case of the Al_n cluster, the negative E_b values increases with an increasing number of Al-atoms due to the increase in the number of bonds. In the case of Al_nC, the $-E_b$ values have increased till n=4 and then remained nearly unchanged for the higher clusters. In the case of Al_nC_2 clusters, the values are found to be gradually decreasing with an increasing number of Al-atoms. Comparing the structures of Al_n and $Al_nC_{1,2}$, the major difference is the replacement of Al-Al bonds with Al-C bonds. The increase in the number of Al-C bonds resulted in the increase in the $-E_b$ values from AlC to Al_4C, which can be correlated to the increase in the number of Al-C bonds from n=1 to 4, respectively. Thereafter, the number of Al-C bonds remained at 4 in the higher clusters.

Additionally, the larger Al-C bond lengths in $Al_{4-7}C$ (SI Figure S1) than that in the smaller clusters suggest weaker bonding in the larger clusters. Therefore, a marginal change in E_b values in Al_{4-7} are expected. In Al_nC_2 molecules, the bond length of the only CC bond increases with an increase in the cluster size (SI Figure S3), and hence the decrease in - E_b for higher n values is observed. Note that the $-E_b$ values of $Al_nC_{1,2}$ converge towards that of the Al_n clusters with increasing n-values because of the limited number of AlC and CC bonds in the clusters. Figure 4B (cationic) and 4C (anionic) show similar observations, suggesting bonding similarity among the species. Figure 4B shows that the average binding energies of the cations are less negative compared to the neutral and anionic clusters, which suggests the lower stability of the cations. In the case of anionic species, $Al_nC_{1-2}^-$, the E_b values (Figure 4C) are higher than the neutral clusters, suggesting the higher stability of the anionic species due to the positive electron affinity of the neutral clusters. The variation of the E_b values of the anionic clusters are found to be similar to that of the neutral clusters.

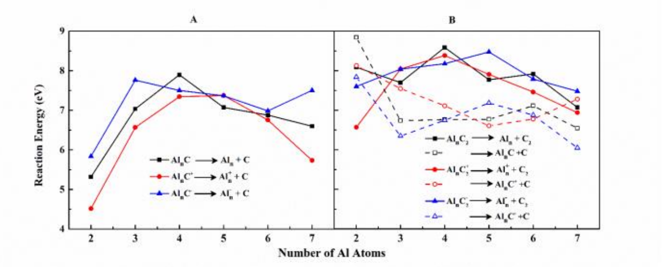

Figure 5: Reaction energies of (A) $Al_{1\text{-}7}C^{0,\pm} \rightarrow Al_n^{0,\pm} + C$, and (B) $Al_{1\text{-}7}C_2^{0,\pm} \rightarrow Al_n^{0,\pm} + C_2$ and $Al_{1\text{-}7}C_2^{0,\pm} \rightarrow Al_nC^{0,\pm} + C$ calculated at B3LYP-D4/def2-TZVPP level of theory.

3.2.2 Dissociation energies

In addition to the binding energy, another critical factor that determines the stability of $Al_nC_{1,2}^{0,\pm}$ (n=1-7) clusters is the dissociation reaction energies ΔE_r. The list of dissociation reactions is mentioned in SI Table S2 and S3. The higher the dissociation reaction energy, suggest that the higher the stability of a structure under dissociation conditions. Figure 5 shows the ΔE_r associated with the removal of C from $Al_{2\text{-}7}C_{1,2}^{0,\pm}$. The ΔE_r values are highly positive, ranging between 5-8 eV/mole. Note that removing a C-atom from $Al_nC_{1\text{-}2}^{0,\pm}$ requires the removal of all AlC and CC (in C_2-doped clusters) bonds. Therefore, in the case of $Al_nC^{0,\pm}$, the ΔE_r values gradually increase till n=4 because of the increase in the number of Al-C bonds in the structures. The lower DE value of Al_7C^+ can be associated with the exceptionally high stability of the dissociation product Al_7^+, as reported earlier that the Al_7^+ is a magic cluster.[58][59] The unusually high DE values of Al_7C^- can be linked with the increased stability of the cluster. In the case of Al_nC_2, the removal of the C_2 unit via $Al_{3\text{-}7}C_2 \rightarrow Al_{3\text{-}7}+C_2$ reactions is found to be energetically unfavorable compared to the elimination of a single carbon atom. Similar to the above, the removal of a C_2 requires the removal of all the Al-C and CC bonds and thus requires more energy than that in the C-elimination reaction. In the case of $Al_2C_2^{0,\pm}$, the removal of the C-atom required the breaking of the acetylenic C≡C bond, and thus the DE values are significantly higher. Overall, the elimination of C and C_2 from $Al_nC^{0,\pm}$ and $Al_nC_2^{0,\pm}$, respectively, are less likely because of several low-energy fragmentation channels (SI Table S3). The dominant dissociation channel is the elimination of Al from the neutral and anionic and Al^+ from cationic species, as described below.

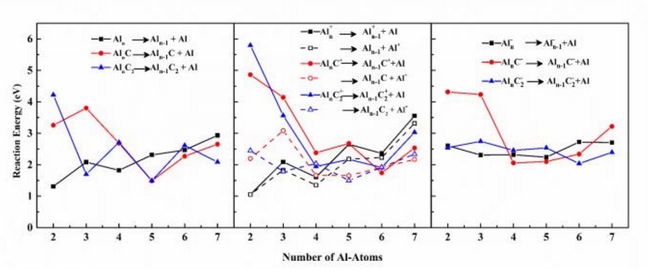

Figure 6: Reaction energies of (A) $Al_{1\text{-}7}C_{0\text{-}2} \rightarrow Al_{n-1}C_{0\text{-}2} + Al$, (B) $Al_{1\text{-}7}C_{0\text{-}2}^+ \rightarrow Al_{n-1}C_{0\text{-}2}^+ + Al$ and $Al_{1\text{-}7}C_{0\text{-}2}^+ \rightarrow Al_{n-1}C_{0\text{-}2} + Al^+$ and (C) $Al_{1\text{-}7}C_{0\text{-}2}^- \rightarrow Al_{n-1}C_{0\text{-}2}^- + Al$ calculated at B3LYP-D4/def2-TZVPP level of theory.

Figures 6A, 6C, and 6B show the dissociation reaction energies ΔE_r associated to the least energetic Al-elimination channels from $Al_nC_{1,2}$ and $Al_nC_{1,2}^-$ (n=1-7), and Al and Al^+ elimination from $Al_nC_{1,2}^+$, respectively. The reaction energy ΔE_r, which was previously reported as incremental binding energy, in the neutral and anionic clusters is defined as $E(Al_nC_m^{0,-1})$-$E(Al_{n-1}C_m^{0,-1})$-E(Al). To further confirm the relative stability among the adjacent clusters, we have used the second-order difference of energy (Δ^2E) parameter, which was calculated as the reaction energy of $2Al_nC_{1,2} \rightarrow Al_{n+1}C_{1,2} + Al_{n-1}C_n$, i.e., $\Delta^2E = E(Al_{n+1}C_{1,2}) + E(Al_{n-1}C_{1,2}) - 2 \times E(Al_nC_{1,2})$. Figures 7A-7C show the Δ^2E of neutral, cationic, and anionic clusters.

The ΔE_r associated with the Al-elimination from Al_nC, as shown in Figure 6A, with n=5, 6, and 7 are 1.49, 2.27, and 2.68 eV, respectively, which are relatively lower than the respective pure Al_n clusters (2.31, 2.47 and 2.93 eV). In the case of smaller Al_nC clusters (n≤4), eliminating the Al atom requires more energy, as all the Al atoms are bound to the carbon atom. In the case of Δ^2E values (Figure 7A), the stability of Al_5C and Al_6C are found to be lower than the smaller clusters. Therefore, the insertion of carbon atoms in $Al_{5\text{-}7}$ clusters generates loosely bound Al atoms. For example, the lower ΔE_r and Δ^2E values of Al_5C (SI Table S3) are due to the easy elimination of the Al attached to the tetrahedral Al_4C moiety (Figure 1).

The variation of ΔE_r values of Al_nC_2 systems (Figure 6A) shows significantly higher values for Al-elimination from the singlet species, i.e., $Al_{2,4,6}C_2$, than the adjacent odd-numbered species with doublet ground states. Similarly, the Δ^2E in Figure 7A shows prominent odd-even parity in Al_nC_2, with higher Δ^2E values in singlet clusters ($Al_{2,4,6}C_2$) than doublet ($Al_{3,5}C_2$) species. The high reaction energy of *l*-Al_2C_2 (Figure 6A) suggests the higher stability of the molecule because of its acetylenic structure. Therefore, the even-numbered Al-clusters possess higher stability due to the singlet ground states.

The reaction $Al_nC_{1,2}^+ \rightarrow Al_{n-1}C_{1,2} + Al^+$ is found to be energetically favourable compared to the Al-elimination channel ($Al_nC_{1,2}^+ \rightarrow Al_{n-1}C_{1,2}^+ + Al$) in the cationic clusters, as shown in Figure 6B. The ΔE_r values of the $Al_{3\text{-}7}C^+$ are nearly similar, as shown in Figure 6B. However, the Δ^2E values of the Al_nC^+ cluster show prominent odd-even parity where the clusters with singlet ground states ($Al_{3,5}C^+$) are more stable than doublet species $Al_{2,4,6}C^+$. Similar to the neutral Al_nC the odd-even parity was not found in the anionic Al_nC clusters.

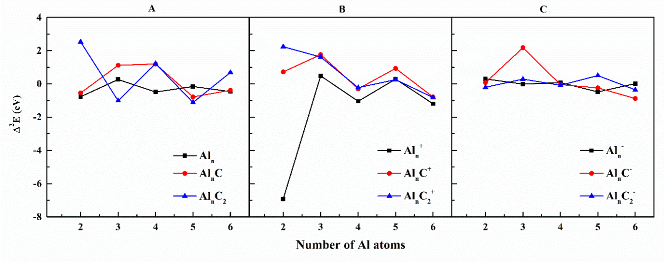

Figure 7: Comparison of second order difference of energy of (A) neutral (B) cationic and (C) anionic Al_nC_m (n=1-7, m=0-2) clusters were calculated at B3LYP-D4/def2-TZVPP level of theory.

Based on both ΔE_r and Δ^2E values (Figures 6 and 7), the stability of Al_nC^+ and $Al_nC_2^+$ are found to be nearly the same for the respective n-values. Overall, the singlet species ($Al_{3,5,7}C_2^+$) are found to be relatively more stable than the $Al_{4,6}$ species. In addition, similar to the neutral species, $Al_2C_2^+$ is found to be highly stable, which is most like because of the acetylenic structure of the molecule. The dissociation energy of $Al_nC_{1,2}^-$ structures via Al-elimination were shown in Figure 6C. In the case of $Al_nC_2^-$, the values show odd-even parity with the higher stability of the odd n-species, which can be linked to the singlet ground state of the molecules. The above can also be confirmed by the Δ^2E values shown in Figure 7C.

3.2.3 Chemical hardness (η) and stability

Another important factor in describing the stability of a metal cluster is the calculated chemical hardness parameter η. This value is correlated to the difference between vertical ionization energy and vertical electron affinity values as η = (IP-EA)/2. The higher η value indicates higher stability, and the lower value indicates higher chemical reactivity. Note that, within the limitations of Koopmans' theorem, the energy of HOMO and LUMO corresponds to the ionization energy and electron affinity. Therefore, the energy gap between the HOMO and LUMO (E_{HL}) can be correlated to the chemical hardness value of a cluster. The calculated values for E_{HL} and η were given in Table 2. The correlation between the parameters is shown in SI Figure S4.

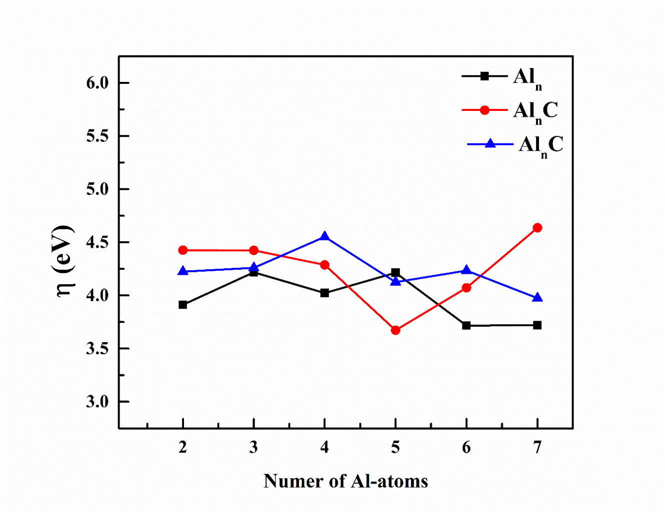

Figure 8: Comparison of Chemical hardness (η) of Al_n, Al_nC, and Al_nC_2

The η $Al_nC_{1,2}$ clusters are higher than the Al_n clusters, except Al_5C, which means the carbon-doped clusters are less reactive compared to pure Al_n clusters, as shown in Figure 8. The odd-even parity is prominent in Al_n clusters with respect to their triplet and doublet states. The $Al_{3,5,7}$ and $Al_{2,4}$ possess doublet and triplet states, respectively, and shows that the doublet species are more stable than the triplet ones. The Al_6 clusters show a smaller η value compared to the adjacent triplet and doublet species because of its singlet ground states. The Al_nC_2 clusters with even n values show singlet ground states, odd n values show doublet ground states, and odd-even parity is observed, which shows that the singlet species are more stable than the doublet ones. In the case of the Al_5C system, the chemical hardness parameter η is lower than the other Al_nC clusters because of the weakly bound fifth Al-atom connected to tetrahedral Al_4C moiety.

3.2.4 Electron affinity and Ionization energy

The electron affinity (EA) is the energy liberated when one electron is added to the neutral molecule. The high electron affinity value indicates the high energy release due to the electron attachment. Both adiabatic (AEA) and vertical electron affinity (VEA) values of A_nC_m clusters were computed and given in Table 2. Vertical EA is measured as the difference between the energy of neutral and anionic clusters without a change in the geometry. The adiabatic EA was measured as the energy difference between the neutral and the anionic cluster with relaxed geometry. The VEA values were found to be slightly higher than AEA values due to the geometry relaxation. The experimental values are found to be in good agreement with the calculated data. For example, the adiabatic EA data of Al_2C_2 and Al_3C_2 clusters were reported experimentally, and our calculated data are in good agreement.[34,35]

The vertical electron detachment energies (VDE) were also calculated and given in Table 2, which were measured as the energy difference between the relaxed geometry of the anionic cluster and the neutral cluster without changing the geometry. The VDE values of Al_nC_{0-2} clusters were found to be increased as the number of aluminium atoms increased and are in good agreement with the experimentally reported data shown in Figure 9A. The Al_nC_2 species shows the odd-even alternation with respect to singlet and doublet states. The above can be explained based on the electronic configuration, where the $Al_{2,4,6}C_2^-$ clusters with doublet states have a π^1-electronic configuration, and the $Al_{3,5,7}C_2^-$ clusters with singlet states with fully filled outer orbitals. So, it is easy to remove an electron from the π^1 orbital rather than the fully filled orbital, which indicates that the singlet $Al_{3,5,7}C_2^-$ clusters are more stable than the doublet $Al_{2,4,6}C_2^-$ clusters. The VDE values show good agreement with the previously reported experimental data of Al_nC (n=3-5)[31–33] and Al_2C_2.[34]

Ionization energy (IE) combined with EA is an essential parameter used to determine the chemical hardness as well as the electronic structure of the clusters. We have calculated vertical and adiabatic ionization energies of Al_nC_{0-2} (n=2-7), which are helpful for the spectroscopic characterization of neutral clusters, are given in Table 2. The IEs of $Al_nC_{1,2}$ (n=2-7) clusters show prominent odd-even parity as observed earlier in the case of chemical hardness and electron affinity, where the singlet $Al_{2,4,6}C_2$ clusters are more stable than the doublet $Al_{3,5,7}C_2$ clusters. The IEs of Al_n clusters do not change much with the addition of an extra aluminium atom. Our calculated IEs show perfect agreement with the experimental data are shown in Figure

9B.[60],[61]

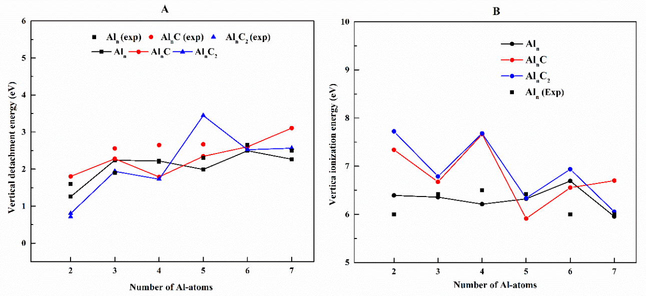

Figure 9: (A) vertical detachment energy VDE (B) vertical ionization energy of Al_n (black squares), Al_nC (red circles) and Al_nC_2 (blue triangles) clusters. The data points without connected line represents the corresponding experimental data.

4. Summary

In this article, we have investigated equilibrium geometries, electronic structures, reactivity, and stability of C/C_2 -doped $Al_n^{0\pm}$ clusters have been systematically studied at B3LYP-D4/def2-TZVPP level of theory. The available experimental and computational data and the predicted most stable structures are in good agreement. The average Al-Al bond length and average binding energy data suggest that the stability of the anionic Al_n clusters is higher than the neutral species, followed by the cationic species. The stability of the clusters was determined with the help of various energy parameters such as average binding energy, dissociation reaction energies, ionization energies, electron affinity, and VDE.

The more negative E_b values of $Al_nC_{1,2}$ indicate that the Doping of carbon increases the stability of the Al_n clusters. It is evident from the structures that some of the Al-Al bonds are replaced by Al-C bonds in Al_nC and Al_nC_2. Similar trends were observed for the cationic $Al_nC_{1,2}^+$ and anionic $Al_nC_{1,2}^-$ clusters. The variation in the E_b values was understood based on the number of Al-C and C-C bonds present in the structure of the cluster.

The dissociation reaction energy (ΔE_r) C_2-elimination reactions from $Al_nC^{0,\pm}$, is found to be energetically unfavourable compared to the elimination of a single carbon atom. The above is due to the elimination of a C_2 requires the removal of all the Al-C and CC bonds and thus requires more energy than that in the C-elimination reaction. The dominant dissociation channel is the elimination of Al from the neutral and anionic and Al^+ from cationic species. In the case of smaller Al_nC clusters ($n \leq 4$), eliminating the Al atom requires more energy, as all the Al atoms are bound to the carbon atom. The stability of Al_5C and Al_6C is found to be lower than the smaller clusters. Therefore, the insertion of carbon atoms in Al_{5-7} clusters generates loosely bound Al atoms. For example, the lower ΔE_r and Δ^2E values of Al_5C are due to the easy elimination of the Al attached to the tetrahedral Al_4C moiety.

The variation of ΔE_r values of Al_nC_2 systems shows significantly higher values for Al-elimination from the singlet species, i.e., $Al_{2,4,6}C_2$, than the adjacent odd-numbered species with doublet ground states. The Al^+-elimination is found to be energetically favorable compared to the Al-elimination channel in the cationic clusters. However, the Δ^2E values of the Al_nC^+ cluster show prominent odd-even parity where the clusters with singlet ground states ($Al_{3,5}C^+$) are more stable than doublet species $Al_{2,4,6}C^+$. Similar to the neutral Al_nC the odd-even parity was not found in the anionic Al_nC clusters. Based on both ΔE_r and Δ^2E values, the stability of Al_nC^+ and $Al_nC_2^+$ are found to be nearly the same for the respective n-values. Overall, the singlet species ($Al_{3,5,7}C_2^+$) are found to be relatively more stable than the $Al_{4,6}$ species. In the case of $Al_nC_2^-$, the values show odd-even parity with the higher stability of the odd n-species, which can be linked to the singlet ground state of the molecules.

The η $Al_nC_{1,2}$ clusters are higher than the Al_n clusters, which means the carbon-doped clusters are less reactive compared to pure Al_n clusters. Based on the chemical hardness parameter, the reactivity of the triplet species is found to be higher than the doublet followed by singlets. The electron affinity, vertical detachment energies, and ionization energies also show a similar trend as seen in the above parameter. The bonding is explained based using molecular orbital diagrams. The current computational investigation demonstrates various factors to understand the stability and reactivity of metal-containing Al_n clusters under extreme conditions, such as combustions or collision-induced reactions. The results of the current investigations are thus highly important for spectroscopy, material, and organometallic chemistry communities.

Supporting Information Available:

The discussion on the isomeric structures, energies and coordinates of the important isomers are given in the Supporting Information document.

Acknowledgment:

JR Thanks UGC for the fellowship, and SM thanks IIT Hyderabad for infrastructure.

References

[1] K.H. Bennemann, J. Koutecky, Small particles and inorganic clusters: proceedings of the third International Meeting on Small Particles and Inorganic Clusters, Freie Universität Berlin, Berlin (West), Germany, 9-13 July 1984, North-Holland Pub. Co., 1985.

[2] S.N. Khanna, P. Jena, Assembling crystals from clusters, Phys. Rev. Lett. 69 (1992) 1664–1667. https://doi.org/10.1103/PhysRevLett.69.1664.

[3] S.N. Khanna, P. Jena, Atomic clusters: Building blocks for a class of solids, Phys. Rev. B. 51 (1995) 13705–13716. https://doi.org/10.1103/PhysRevB.51.13705.

[4] H. Yang, Y. Zhang, H. Chen, Dissociation of H2 on carbon doped aluminum cluster Al 6C, J. Chem. Phys. (2014) 141, 064302. https://doi.org/10.1063/1.4891860.

[5] F. Dong, S. Heinbuch, Y. Xie, J.J. Rocca, E.R. Bernstein, Experimental and theoretical study of neutral AlmCn and AlmCnHx clusters, Phys. Chem. Chem. Phys. 12 (2010) 2569–2581. https://doi.org/10.1039/b922026g.

[6] A. Nakajima, T. Kishi, T. Sugioka, Y. Sone, K. Kaya, Mass distributions of aluminum negative cluster ions and their binary cluster ions mixed with a carbon atom, Chem. Phys. Lett. 177 (1991) 297–300. https://doi.org/10.1016/0009-2614(91)85034-T.

[7] B.C. Guo, K.P. Kerns, A.W. Castleman Jr., Ti8C12+-metallo-carbohedrenes: a new class of molecular clusters?, Science (80-.). 255 (1992) 1411.

[8] B. Wu, F. Wu, P. Wang, A. He, H. Wu, Ignition and Combustion of Hydrocarbon Fuels Enhanced by Aluminum Nanoparticle Additives : Insights from Reactive Molecular Dynamics Simulations, J. Phys. Chem. (2021)125, 11359−11368. https://doi.org/10.1021/acs.jpcc.1c01435.

[9] M.S. Gad, S.M.A. Razek, P. V Manu, S. Jayaraj, Experimental investigations on diesel engine using alumina nanoparticle fuel additive, Advances in Mechanical Engineering 2021, 13 1–16. https://doi.org/10.1177/1687814020988402.

[10] N. Vetkasov, L. Khudobin, V. Sapunov, S. Varlamov, Obtaining, microstructure and microhardness of carbon-doped aluminomatrix composites, Mater. Today Proc. 38 (2021) 1706–1710. https://doi.org/10.1016/j.matpr.2020.08.230.

[11] M.S. Kulkarni, K.P. Muthe, N.S. Rawat, D.R. Mishra, M.B. Kakade, S. Ramanathan, S.K. Gupta, B.C. Bhatt, J. V. Yakhmi, D.N. Sharma, Carbon doped yttrium aluminum garnet (YAG:C)-A new phosphor for radiation dosimetry, Radiat. Meas. 43 (2008) 492–496. https://doi.org/10.1016/j.radmeas.2007.10.039.

[12] X.B. Yang, J. Xu, H.J. Li, Q.Y. Bi, L.B. Su, Y. Cheng, Q. Tang, Thermoluminescence properties of carbon doped Y3 Al5 O12 (YAG) crystal, J. Appl. Phys. 106 (2009), 033105. https://doi.org/10.1063/1.3194794.

[13] Z. Abdeveiszadeh, E. Shakerzadeh, S. Noorizadeh, Computational screening of carbon monoxide (CO) adsorption over neutral and charged Al7 clusters, Heliyon. 5 (2019) e01762. https://doi.org/10.1016/j.heliyon.2019.e01762.

[14] R. Wang, D. Zhang, W. Sun, Z. Han, C. Liu, A novel aluminum-doped carbon nanotubes sensor for carbon monoxide, J. Mol. Struct. THEOCHEM. 806 (2007) 93–97. https://doi.org/10.1016/j.theochem.2006.11.012.

[15] Q. Li, G. Yang, K. Wang, X. Wang, Preparation of carbon-doped alumina beads and their application as the supports of Pt–Sn–K catalysts for the dehydrogenation of propane, React. Kinet. Mech. Catal. 129 (2020) 805–817. https://doi.org/10.1007/s11144-020-01753-4.

[16] Liandi Li, Meysam Najafi, Investigation of Potential of Oxygen Reduction Reaction at Aluminum Doped Carbon Nanocage (Al-C72) as a Catalyst, Russ. J. Phys. Chem. B. 14 (2020) 40–44. https://doi.org/10.1134/S1990793120010248.

[17] M. Sun, X. Wang, X. Shang, X. Liu, M. Naja, Journal of Molecular Graphics and Modelling Investigation of performance of aluminum doped carbon nanotube (8 , 0) as adequate catalyst to oxygen reduction reaction, Journal of Molecular Graphics and Modelling 92 (2019) 123e130. https://doi.org/10.1016/j.jmgm.2019.07.010.

[18] A.S. Lozhkomoev, E.A. Glazkova, N. V Svarovskaya, O. V Bakina, O. Sergey, A.S. Lozhkomoev, E.A. Glazkova, N. V Svarovskaya, Specific Features of Aluminum Nanoparticle Water and Wet Air Oxidation, AIP Conference Proceedings1683 (2015), 020128. https://doi.org/10.1063/1.4932818.

[19] B. Zeng, S. Wang, Y. Gao, G. Li, W. Tian, J. Meeprasert, H. Li, H. Xie, F. Fan, R. Li, C. Li, Interfacial Modulation with Aluminum Oxide for Efficient Plasmon-Induced Water Oxidation, Adv. Funct. Mater. 2005688 (2020) 1–8. https://doi.org/10.1002/adfm.202005688.

[20] S. Anatolievna, S. Vladislavovich, A. Alexandrovich, U. Teipel, Air and water oxidation of aluminum fl ake particles, Powder Technology 307 (2017) 184–189. https://doi.org/10.1016/j.powtec.2016.12.009.

[21] B.K. Rao, P. Jena, Energetics and electronic structure of carbon doped aluminum clusters, J. Chem. Phys. 115 (2001) 778–783. https://doi.org/10.1063/1.1379973.

[22] T. Kamiński, H.S.P. Müller, M.R. Schmidt, I. Cherchneff, K.T. Wong, S. Brünken, K.M. Menten, J.M. Winters, C.A. Gottlieb, N.A. Patel, study of dust in Mira (o Ceti), Astron. Astrophys. 599 (2017) A59. https://doi.org/10.1051/0004-6361/201629838.

[23] R.S. Furuya, C.M. Walmsley, K. Nakanishi, P. Schilke, R. Bachiller, Interferometric observations of FeO towards Sagittarius B2 . A&A 409, (2003)L21–L24. https:// DOI: 10.1051/0004-6361:20031304

[24] E.D. Tenenbaum, L.M. Ziurys, Exotic metal molecules in oxygen-rich envelopes: Detection of ALOH (X 1Σ+) in VY Canis Majoris, Astrophys. J. Lett. 712 (2010) 93–97. https://doi.org/10.1088/2041-8205/712/1/L93.

[25] T. Kami, Molecular dust precursors in envelopes of oxygen-rich AGB stars and red supergiants, International Astronomical Union 343(2018) 108-118 https://doi.org/10.1017/S1743921318006038

[26] L.N. Zack, D.T. Halfen, L.M. Ziurys, Detection of FeCN (X 4 Δ i) in IRC+10216: A new interstellar molecule, Astrophys. J. Lett. 733 (2011). https://doi.org/10.1088/2041-8205/733/2/L36.

[27] M.A. Anderson, L.M. Ziurys, The Millimeter/Submillimeter Spectrum and Rotational Rest Frequencies of MgCH3 Astrophys. J. 452 (1995) 1–4. https://doi.org/10.1086/309733.

[28] C. Apetrei, A.E.W. Knight, E. Chasovskikh, E.B. Jochnowitz, H. Ding, J.P. Maier, Gas phase electronic spectrum of T-shaped AlC2 radical, J. Chem. Phys. 131 (2009). https://doi.org/10.1063/1.3186758.

[29] J. Yang, R.H. Judge, D.J. Clouthier, Pulsed discharge jet electronic spectroscopy of the aluminum dicarbide (AlC2) free radical, J. Chem. Phys. 135 (2011). https://doi.org/10.1063/1.3638049.

[30] D.T. Halfen, L.M. Ziurys, The pure rotational spectrum of the T-shaped AlC2 radical (: X 2A1), Phys. Chem. Chem. Phys. 20 (2018) 11047–11052. https://doi.org/10.1039/c7cp08613j.

[31] A.I. Boldyrev, Combined photoelectron spectroscopy and ab initio study of the hypermetallic Al3C molecule, J. Chem. Phys. 110 (1999) 8980–8985. https://doi.org/10.1063/1.478816.

[32] X. Li, L.S. Wang, A.I. Boldyrev, J. Simons, Tetracoordinated planar carbon in the Al4C- anion. A combined photoelectron spectroscopy and ab initio study, J. Am. Chem. Soc. 121 (1999) 6033–6038. https://doi.org/10.1021/ja9906204.

[33] A.I. Boldyrev, J. Simons, X. Li, L.S. Wang, The electronic structure and chemical bonding of hypermetallic Al5C by ab initio

calculations and anion photoelectron spectroscopy, J. Chem. Phys. 111 (1999) 4993–4998. https://doi.org/10.1063/1.479744.

[34] N.A. Cannon, A.I. Boldyrev, X. Li, L.-S. Wang, The electronic structure and chemical bonding of aluminum acetylide: Al2C2 and Al2C2−: An experimental and theoretical investigation, J. Chem. Phys. 113 (2000) 2671–2679. https://doi.org/10.1063/1.1305881.

[35] X. Li, L.S. Wang, N.A. Cannon, A.I. Boldyrev, Electronic structure and chemical boning in nonstoichiometric molecules: Al3X2-(X=C,Si,Ge). A photoelectron spectroscopy and ab initio study, J. Chem. Phys. 116 (2002) 1330–1338. https://doi.org/10.1063/1.1429652.

[36] C.J. Zhang, P. Wang, X.L. Xu, H.G. Xu, W.J. Zheng, Photoelectron spectroscopy and theoretical study of AlnC5−/0(n= 1-5) clusters: structural evolution, relative stability of star-like clusters, and planar tetracoordinate carbon structures, Phys. Chem. Chem. Phys. 23 (2021) 1967–1975. https://doi.org/10.1039/d0cp06081j.

[37] J. Zhao, B. Liu, H. Zhai, R. Zhou, G. Ni, Z. Xu, Mass spectrometric and first principles study of AlnC- clusters, Solid State Commun. 122 (2002) 543–547. https://doi.org/10.1016/S0038-1098(02)00210-7.

[38] K. Tsuruoka, K. Koyasu, S. Hirabayashi, M. Ichihashi, T. Tsukuda, Size-Dependent Polymorphism in Aluminum Carbide Cluster Anions AlnC2-: Formation of Acetylide-Containing Structures, J. Phys. Chem. C. 122 (2018) 8341–8347. https://doi.org/10.1021/acs.jpcc.7b12767.

[39] F.Y. Naumkin, Flat-structural motives in small alumino-carbon clusters C nAln, (n = 2-3, m = 2-8), J. Phys. Chem. A. 112 (2008) 4660–4668. https://doi.org/10.1021/jp711230x.

[40] B.I. Loukhovitski, A.S. Sharipov, A.M. Starik, Physical and thermodynamic properties of AlnCm clusters: Quantum-chemical study, J. Phys. Chem. A. 119 (2015) 1369–1380. https://doi.org/10.1021/jp5108087.

[41] C. Ashman, S.N. Khanna, M.R. Pederson, Reactivity of Al n C clusters with oxygen: Search for new magic clusters, Chem. Phys. Lett. 324 (2000) 137–142. https://doi.org/10.1016/S0009-2614(00)00569-8.

[42] D.Y. Zubarev, A.I. Boldyrev, Appraisal of the performance of nonhybrid density functional methods in characterization of the Al 4 C molecule, J. Chem. Phys. 122 (2005). https://doi.org/10.1063/1.1873532.

[43] N. Du, H. Yang, H. Chen, Covalent vs Ionic Bonding in Al-C Clusters. J. Phys. Chem. A 121 (2017), 4009−4018 https:// DOI: 10.1021/acs.jpca.7b01532

[44] Q. Sun, Q. Wang, X.G. Gong, V. Kumar, Y. Kawazoe, Structures and stability of Al7C and Al7N clusters, Eur. Phys. J. D. 18 (2002) 77–81. https://doi.org/10.1140/e10053-002-0009-4.

[45] Y. Pei, W. An, K. Ito, P.V.R. Schleyer, C.Z. Xiao, Planar pentacoordinate carbon in CAI5+: A global minimum, J. Am. Chem. Soc. 130 (2008) 10394–10400. https://doi.org/10.1021/ja803365x.

[46] Y.B. Wu, H.G. Lu, S.D. Li, Z.X. Wang, Simplest neutral singlet C2e4 (E = Al, Ga, In, and Tl) global minima with double planar tetracoordinate carbons: Equivalence of C2 moieties in C2e4 to carbon centers in CAl42- and CAl5+, J. Phys. Chem. A. 113 (2009) 3395–3402. https://doi.org/10.1021/jp8099187.

[47] S.J. Wang, X.Y. Kuang, C. Lu, Y.F. Li, Y.R. Zhao, Geometries, stabilities, and electronic properties of Pt-group-doped gold clusters, their relationship to cluster size, and comparison with pure gold clusters, Phys. Chem. Chem. Phys. 13 (2011) 10119–10130. https://doi.org/10.1039/c0cp02506b.

[48] J. Zhao, J. Wang, G. Wang, Structure and electronic properties of (formula presented) (formula presented) clusters from density-functional theory, Phys. Rev. B - Condens. Matter Mater. Phys. 64 (2001) 1–5. https://doi.org/10.1103/PhysRevB.64.205411.

[49] X. Feng, Y. Luo, Structure and Stability of Al-Doped Boron Clusters by the Density-Functional Theory, J. Phys. Chem. A, 111(2007), 2420-2425.

[50] F. Furche, R. Ahlrichs, C. Hättig, W. Klopper, M. Sierka, F. Weigend, No Title, Turbomole. WIREs Comput. Mol. Sci. 4 (2014) 91.

[51] A.D. Becke, Density-functional thermochemistry. III. The role of exact exchange, J. Chem. Phys. 98 (1993) 5648–5652. https://doi.org/10.1063/1.464913.

[52] L.P. Tan, D. Die, B.X. Zheng, Growth mechanism, electronic properties and spectra of aluminum clusters, Spectrochim. Acta - Part A Mol. Biomol. Spectrosc. 267 (2022) 120545. https://doi.org/10.1016/j.saa.2021.120545.

[53] S. Paranthaman, K. Hong, J. Kim, D.E. Kim, T.K. Kim, Density functional theory assessment of molecular structures and energies of neutral and anionic Aln (n = 2-10) clusters, J. Phys. Chem. A. 117 (2013) 9293–9303. https://doi.org/10.1021/jp4074398.

[54] N. Du, H. Yang, H. Chen, Covalent versus Ionic Bonding in Al-C Clusters, J. Phys. Chem. A. 121 (2017) 4009–4018. https://doi.org/10.1021/acs.jpca.7b01532.

[55] L.I. Gui-fa, L.U. Shi-qiang, P. Ping, Theoretical Study of Geometric Structures, Chinese Journal of Structural Chemistry 31(2012), 582-590.

[56] B.J. Irving, F.Y. Naumkin, A computational study of “Al-kanes” and “Al-kenes,” Phys. Chem. Chem. Phys. 16 (2014) 7697–7709. https://doi.org/10.1039/c3cp54662d.

[57] F.Y. Naumkin, Flat-structural Motives in Small Alumino - Carbon Clusters C n Al m (n) 2 - 3 , m) 2 - 8), Phys. Chem. A, 112 (2008) 4660–4668. https://doi.org/10.1021/jp711230x

[58] V.O. Kiohara, E.F.V. Carvalho, C.W.A. Paschoal, F.B.C. Machado, O. Roberto-Neto, DFT and CCSD(T) electronic properties and structures of aluminum clusters: Alnx (n = 1-9, x = 0, ±1), Chem. Phys. Lett. 568–569 (2013) 42–48. https://doi.org/10.1016/j.cplett.2013.03.005.

[59] Y. Erdogdu, Ş. Erkoç, Evolution of the electronic structure and properties of charged titanium doped aluminum nanoclusters, Comput. Mater. Sci. 79 (2013) 599–610. https://doi.org/10.1016/j.commatsci.2013.07.010.

[60] K.E. Schriver, J.L. Persson, E.C. Honea, R.L. Whetten, Electronic shell structure of group-IIIA metal atomic clusters, Phys.

Rev. Lett. 64 (1990) 2539–2542. https://doi.org/10.1103/PhysRevLett.64.2539.

[61] D.M. Cox, D.J. Trevor, R.L. Whetten, A. Kaldor, Aluminum clusters: Ionization thresholds and reactivity toward deuterium, water, oxygen, methanol, methane, and carbon monoxide, J. Phys. Chem. 92 (1988) 421–429. https://doi.org/10.1021/j100313a036.